soil systems

MDPI

Article

A Novel Approach for High-Frequency *in-situ* Quantification of Methane Oxidation in Peatlands

Cecilie Skov Nielsen *, Niles J. Hasselquist, Mats B. Nilsson, Mats Öquist, Järvi Järveoja and Matthias Peichl

Department of Forest Ecology and Management, Swedish University of Agricultural Sciences, Skogsmarksgränd, 90183 Umeå, Sweden; niles.hasselquist@slu.se (N.J.H.); mats.b.nilsson@slu.se (M.B.N.); mats.oquist@slu.se (M.Ö.); jarvi.jarveoja@slu.se (J.J.); matthias.peichl@slu.se (M.P.)

* Correspondence: cecilie.skov.nielsen@slu.se; Tel.: +46-907-868172

Received: 5 October 2018; Accepted: 14 December 2018; Published: 31 December 2018

Abstract: Methane (CH_4) oxidation is an important process for regulating CH_4 emissions from peatlands as it oxidizes CH_4 to carbon dioxide (CO_2). Our current knowledge about its temporal dynamics and contribution to ecosystem CO_2 fluxes is, however, limited due to methodological constraints. Here, we present the first results from a novel method for quantifying *in-situ* CH_4 oxidation at high temporal resolution. Using an automated chamber system, we measured the isotopic signature of heterotrophic respiration (CO_2 emissions from vegetation-free plots) at a boreal mire in northern Sweden. Based on these data we calculated CH_4 oxidation rates using a two-source isotope mixing model. During the measurement campaign, 74% of potential CH_4 fluxes from vegetation-free plots were oxidized to CO_2, and CH_4 oxidation contributed 20 $\pm$ 2.5% to heterotrophic respiration corresponding to 10 $\pm$ 0.5% of ecosystem respiration. Furthermore, the contribution of CH_4 oxidation to heterotrophic respiration showed a distinct diurnal cycle being negligible during nighttime while contributing up to 35 $\pm$ 3.0% during the daytime. Our results show that CH_4 oxidation may represent an important component of the peatland ecosystem respiration and highlight the value of our method for measuring *in-situ* CH_4 oxidation to better understand carbon dynamics in peatlands.

Keywords: Methane oxidation; peatland; heterotrophic respiration; carbon; CO_2; mire

1. Introduction

Northern peatlands are an important component of the global carbon (C) cycle, as they are sinks of carbon dioxide (CO_2) and store about one third of the global soil organic C stock [1]. However, northern peatlands also emit the potent greenhouse gas methane (CH_4) at a rate that depends on the balance between CH_4 production and oxidation of CH_4 to CO_2. Detailed knowledge of *in-situ* CH_4 production and oxidation dynamics is thus key for understanding the contribution of CH_4 from northern peatlands to the atmosphere. Furthermore, as these processes are sensitive to climatic factors [2–4], this understanding is even more crucial in order to accurately predict the role of northern peatlands for the atmospheric radiative forcing under a changing climate.

No studies to our knowledge have measured *in-situ* CH_4 oxidation continuously with high temporal resolution in predominantly methanogenic systems, e.g., peatlands, in the field. Furthermore, current studies do not estimate the contribution of CO_2 resulting from CH_4 oxidation to total ecosystem respiration (ER, abbreviations are listed in Table 1), and thus our understanding of the importance of this process in relation to the other CO_2 component fluxes is limited. Most peatland CO_2 models assume that all heterotrophic respiration (R_h) comes from soil organic matter (SOM) mineralization [5–8] while ignoring the contributions from CH_4 oxidation. Meanwhile, those models that estimate *in-situ* CH_4 oxidation lack data for validation [9]. This could potentially result in false parametrization and

model predictions and overestimation of SOM mineralization with impacts on the modeling of the C balance. Another important limitation of previous studies is that they do not measure CH_4 oxidation continuously and with high temporal resolution, and as a result we know little of the temporal variation of CH_4 oxidation on both diurnal and seasonal time scales. This might further affect model prediction and estimation, particularly if input data is measured only during daytime and/or during the peak growing season. These issues therefore highlight the need for high temporal resolution CH_4 oxidation data in order to support process-based model development and to further improve our understanding of the peatland C cycle.

Table 1. List of abbreviations used in the article.

Term	Abbreviation
Concentration of headspace CH_4 at time 0 in the incubation experiment for the fractionation factor	$[CH_4]_0$
Concentration of headspace CH_4 at time t in the incubation experiment for the fractionation factor	$[CH_4]_t$
Ecosystem respiration	ER
Fractional contribution of CH_4 oxidation to heterotrophic respiration	f_{CH4}
Kinetic fractionation factor	α
Heterotrophic respiration	R_h
Isotopic ^{13}C signature	$\delta^{13}C$
Isotopic ^{13}C signature of ecosystem respiration	$\delta^{13}C_{ER}$
Isotopic ^{13}C signature of headspace CH_4 at times 0 in the incubation experiment for the fractionation factor	$\delta^{13}C_{CH4,0}$
Isotopic ^{13}C signature of headspace CH_4 at times t in the incubation experiment for the fractionation factor	$\delta^{13}C_{CH4,t}$
Isotopic ^{13}C signature of heterotrophic respiration	$\delta^{13}C_{Rh}$
Isotopic ^{13}C signature of pore water CH_4	$\delta^{13}C_{CH4,pw}$
Isotopic ^{13}C signature of organic matter	$\delta^{13}C_{OM}$
Net ecosystem exchange	NEE
Organic matter	OM
Permil fractionation factor	Δ
Relative CH_4 oxidation %	$\%CH_{4oxi}$
Soil organic matter	SOM

Current methods for estimating CH_4 oxidation in peatlands include laboratory incubations [10–12], often in combination with oxidation inhibitors [13–15], stable isotope techniques [10,16–19], methane profiles [20] and gas push-pull tests [21] which all have their strengths and weaknesses. For instance, the disadvantage of incubations is that they may estimate oxidation potentials instead of actual *in-situ* rates. Meanwhile, oxidation inhibitors are intrusive, do not allow for repeated measurements, and may partly inhibit CH_4 production [22,23]. The use of natural abundance stable isotope techniques is promising, although these techniques have traditionally been based on manual sampling which limits the spatial and temporal resolution of these measurements. In addition, natural abundance approaches depend on reliable estimates of the fractionation factors for CH_4 oxidation and diffusion [18,24]. Thus, there is a need for new methods that overcome these limitations and allow *in-situ* measurements of CH_4 oxidation at high temporal scales to better parameterize C and greenhouse gas dynamics in peatlands.

This study aims at developing a method for continuous high-frequency estimates of peatland CH_4 oxidation and the proportion of R_h that emanates from CH_4 oxidation. In spring 2014, we established an experimental setup in the field with automated flux chambers connected to a Picarro G1101-*i* isotopic CO_2 analyzer (Picarro Inc., Santa Clara, CA, USA) in an oligotrophic, minerogenic mire in northern Sweden. We measured massfluxes and isofluxes of ER and R_h (from plots with all photosynthetic biomass removed). By combining the isotopic signature ($\delta^{13}C$) of R_h, organic matter (OM) and pore water CH_4 in a two-source mixing model, we were for the first time able to partition the CO_2 originating from heterotrophic respiration into CO_2 resulting from CH_4 oxidation and mineralization of OM.

2. Materials and Methods

2.1. Site Description

The field site is an oligotrophic, minerogenic mire, Degerö Stormyr (64°11′ N, 19°33′ E), located near the town of Vindeln, Västerbotten County, Northern Sweden. The average annual temperature and average annual precipitation of the World Meteorological Organization (WMO) reference normal period 1961–1990 is 1.2 °C and 523 mm respectively (Table 2) [25]. Long-term net ecosystem exchange (NEE) is −58 g C m^{-2} $year^{-1}$ [26], average growing season CH_4 emission rates are *ca.* 1 to 5 mg CH_4 m^{-2} h^{-1} [27], and the net ecosystem carbon balance is *ca.* −20 to −27 g C m^{-2} $year^{-1}$ [28]. Approximately half of the precipitation comes as snow and snow cover lasts for about six months (November to April). The peat layer is on average 3 to 4 m deep and the growing season water table generally varies between ca. 0 and 25 cm [26,28]. The vegetation consists mainly of *Sphagnum majus* Russ. C. Jens., *Sphagnum balticum* Russ. C. Jens., and *Sphagnum lindbergii* Schimp. Ex Lindb, *Eriophorum vaginatum* L., *Trichophorum cespitosum* L. Hartm., *Vaccinium oxycoccos* L., *Andromeda polifolia* L., *Rubus chamaemorus* L. [29].

Table 2. Climate and soil properties at Degerö Stormyr.

Properties	Value
Mean annual temperature	1.2 °C [25]
Mean annual precipitation	523 mm [25]
Growing season mean water table level	−4.1 cm [30]
Average depth of peat layer	3–4 m [28]
Peat C:N ratio [1]	68.9 ± 1.9

[1] 0–30 cm depth.

2.2. Experimental Setup

The experimental setup was established in spring 2014 and consists of four replicate blocks containing three plots (1 × 1 m) each with different treatments, resulting in a total of 12 plots. Thus, each treatment/measurement type has four replicates. Each plot is equipped with an automated chamber (45 × 45 cm, 15 cm high) for flux measurements. A detailed description of the automated chamber system is provided by Järveoja et al. 2018 [30]. Briefly, two plots in each block are undisturbed where one is used for measurements of NEE using a transparent chamber and the other for measurements of ER using a dark chamber. In the third plot within each block, the aboveground vegetation, including the green parts (i.e., ~upper 5 cm) of the *Sphagnum* mosses, was removed in autumn 2013, and a 30 cm deep trench was cut along the plot sides using a handheld saw to prevent root activity inside the plots. These plots were used for measurements of CO_2 from heterotrophic activity (R_h) with a dark chamber. CH_4 fluxes were also measured at all plots. Each automatic flux chamber has measurements of air temperature 10 cm above the peat surface, and soil temperature at 2 and 10 cm depth. A water level sensor is also placed in each block.

2.3. Measurements of Mass and Isotopes of CH_4 and CO_2

Fluxes of CO_2 and CH_4 mass as well as the $\delta^{13}C$ signature of the CO_2 concentrations were measured in the period of 18 to 27 July 2014. Massfluxes of CO_2 (NEE, ER, R_h) and CH_4 were measured using a greenhouse gas analyzer (model GGA-24EP, Los Gatos Research (LGR) Inc., San Jose, CA, USA) connected in a closed loop to the chambers. Isofluxes and massfluxes, used for Keeling plots, were measured using a Picarro G1101-*i* (Picarro Inc., CA, USA) placed downstream of the LGR. Analytical precision *for in-situ* carbon isotope analyses using the Picarro 1101-*i* instrument was 0.2‰ based on repeated analysis of known isotopic standards. An external pump was connected to the loop to provide continuous airflow. Chamber closure time lasted 18 min and was preceded and followed by one-minute flushing of the tubes with ambient air before onset of next measurement. Measurements

took one hour per block and thus four hours for one round of measurements. The mean time of each four-hour measurement round is used to designate the measurement time point for a four-hour mean flux. For example, the measurement round taking place from 00.00 to 04:00 a.m. is reported for the time point 02:00 a.m.

2.4. Isotopic Signature of Soil Organic Matter and Pore Water CH_4

In order to obtain the $\delta^{13}C$ signature of soil organic matter ($\delta^{13}C_{OM}$), eight peat cores from 0 to 30 cm depth, which represents the area of highest potential CH_4 production and oxidation activity [31], were collected from the mire in October 2015. The cores were cut into 2 cm sections and freeze-dried. The 2 cm sections were then ground in a ball mill and analyzed for $\delta^{13}C$ signature on an elemental analyzer (Flash EA 2000, Thermo Scientific, Bremen, Germany) coupled to a continuous flow isotope ratio mass spectrometer (IRMS, Delta V Advantage, Thermo Scientific, Bremen, Germany). The standard deviation based on analysis of standards was <0.15‰ for $\delta^{13}C$.

On 3 and 27 August 2015, pore water was collected at 20 and 30 cm just outside the chamber frames in the non-vegetated plots and the vegetated plots used for dark measurements, as well as one location in the middle of the four blocks (n = 30). 2 mL of pore water was sampled using a syringe and transferred to N_2 flushed vials. Subsequently, 2 mL of gas was removed from the vials in order to equalize the pressure. The samples were stored at 5 °C until analysis for $\delta^{13}C$ signature of CH_4 ($\delta^{13}C_{CH4,pw}$) on a Precon (Thermo Scientific, Bremen, Germany) and a gasbench (GasBench II, Thermo Scientific, Bremen, Germany) connected to a continuous flow IRMS (Delta V Advantage, Thermo Scientific, Bremen, Germany) on 28 and 29 September 2015. The standard deviation based on analysis of standards was <0.3‰ for $\delta^{13}C$.

2.5. Incubation Experiment to Determine the Fractionation Factor for CH_4 Oxidation

Four cores of 10 × 10 cm and 20 cm deep were collected in the Degerö mire on 8 October 2017. The cores were divided into four depths 0–5, 5–10, 10–15 and 15–20 cm below live vegetation, put in zip lock bags, brought back to the lab and placed in a freezer (−18 °C). Samples were kept frozen for two months and then preincubated at 4 °C for a month. After preincubation, 10 g field moist peat material from each sub core was transferred to 160 mL airtight glass bottles. Three replicates were made of each sample (to be incubated at three different temperatures) giving a total of 48 bottles (i.e., one sample per layer per core for each temperature). In addition, nine blanks (bottles containing 10 mL water as an analogue for field moist peat) were prepared. All bottles had ambient air inside and were given 0.05 mL pure CH_4 to feed the methanotrophs, and placed at 5 °C.

Six days after addition of CH_4, two replicate batches of bottles were placed at 10 and 15 °C respectively, while one replicate batch remained at 5 °C. After an additional three days, the bottles were flushed with technical air and given 0.12 mL pure CH_4, thereby raising headspace to app. 1000 ppm. Immediately after injecting CH_4, 0.5 mL of the headspace was sampled and transferred to 12 mL vials containing helium. Further headspace samples were taken at six, 12, 24, and 48 h and additionally at 96 h for the 0–5 cm interval in order to trace the oxidation rate (i.e., the decrease in headspace CH_4 concentration over time, and the concurrent change in $\delta^{13}C$ signature of the CH_4). For ^{13}C isotope analysis of CH_4 in the gas samples, a Finnigan MAT PreCon unit (Thermo Scientific, Bremen, Germany) was used for automated sample conversion and concentration. Briefly, sample CO_2 was removed by chemical adsorption succeeded by Pt-catalyzed oxidation of the CH_4-component to CO_2 that was subsequently trapped by duplicated cryogenic (liquid N_2) focusing. The isotopic analysis took place upon separation on a GC (HP 6890, equipped with 25 m long PoraPlot Q fused-silica column (32 mm i.d.), operated at 40 °C) coupled in continuous flow-mode to a Finnigan MAT Delta PLUS isotope ratio mass spectrometer. At the 24-h sampling, an additional 0.5 mL of the headspace was taken out and transferred to a 22 mL vial, where the concentration of CH_4 was determined on a gas chromatograph in order to preliminarily assess the oxidation rate and hence the required incubation

time (data not shown). By the end of the experiment, the peat samples were dried for 48 h at 60 degrees and weighed for determination of dry weight.

2.6. Flux Calculation and Estimation of Flux Isotopic Signature

Massfluxes of NEE, ER, R_h and CH_4 were calculated from the linear change in gas concentration within the chamber headspace over time using the ideal gas law [30]. The linear slope was determined based on 10 concentration records over a 1 min 40 s calculation window (each record representing a 10 s mean of the 1 Hz sampling) moving stepwise (with one-point increments) over the chamber closure period. From these individual slopes, the one with the highest coefficient of determination (R^2) was selected as the final slope for each flux measurement. All fluxes with an $R^2 \geq 0.90$ ($p < 0.001$) were accepted giving a total of 428 CO_2 flux measurements and 437 CH_4 flux measurements over the ten-day period.

The $\delta^{13}C$ source signature of respired CO_2 (corresponding to the $\delta^{13}C$ signature of the source material) was determined using the Keeling plot approach [32]. The Picarro G1101-*i* logged measurements approximately every four seconds. From these data, one-minute averages were generated. Disregarding the first one minute average, we used linear regression analysis of $\delta^{13}C$ and $1/[CO_2]$ for the remaining 17 min, with the y-axis intercept corresponding to the ^{13}C signature of respired soil CO_2. Intercepts were excluded for regressions with slopes not significantly different from 0 ($p > 0.05$) and if the slopes were between -0.25 ppm min^{-1} and 0.25 ppm min^{-1} due to the uncertainty in Keeling estimates associated with very small fluxes.

2.7. Calculation of Fractionation Factor for CH_4 Oxidation

To account for preferential use of ^{12}C over ^{13}C by methanotrophs [33,34], we used a kinetic fractionation factor for CH_4 oxidation (hereafter referred to as "fractionation factor" or α). The fractionation factor describes the fractionation against the heavy isotope, where $\alpha = 1$ means no fractionation and $\alpha > 1$ means that fractionation is occurring with product becoming depleted in the heavy isotope and the substrate becoming enriched. α was calculated by the following equations [24] based on data from the incubation experiment:

$$\alpha = \frac{1}{(m+1)}, \tag{1}$$

where m is:

$$m = \frac{\delta^{13}C_{CH4,t} - \delta^{13}C_{CH4,0}}{\ln \frac{[CH_4]_t}{[CH_4]_0}}, \tag{2}$$

and $\delta^{13}C_{CH4,0}$ and $\delta^{13}C_{CH4,t}$ designates the $\delta^{13}C$ signature of the headspace CH_4 at times 0 and t, and $[CH_4]_0$ and $[CH_4]_t$ is the concentration of the headspace CH_4 at times 0 and t. In practice, since we had more than two time points, m was calculated as the slope of a linear regression between the difference in isotopic signatures ($\delta^{13}C_t$–$\delta^{13}C_0$) and natural logarithm of the fraction between remaining and initial headspace CH_4 concentration ($\ln([CH_4]_t/[CH_4]_0)$ [24]. The permil fractionation factor Δ could then be calculated from the α [35]:

$$\Delta = \frac{\alpha - 1}{1000}. \tag{3}$$

CH_4 oxidation rates were also calculated for the incubations, using linear regression. Only significant fractionation factors (slope different from 0, $p < 0.05$) with a corresponding flux <0 were included in the analysis.

2.8. Mixing Model

The fractional contribution of CH_4 oxidation and OM mineralization to total R_h was calculated using a two-source mixing model [35]:

$$f_{CH4} = \frac{\delta_{sample} - \delta^{13}C_{OM}}{\delta^{13}C_{CH4,pw} - \Delta - \delta_{OM}}, \quad (4)$$

where f_{CH4} is the fraction of the heterotrophic respiration contributed by oxidation of CH_4, δ_{sample} is the $\delta^{13}C$ signature of the heterotrophic respiration, $\delta^{13}C_{CH4,pw}$ is the isotopic signature of dissolved CH_4 in pore water, and $\delta^{13}C_{OM}$ is the isotopic signature of the OM. We used the mean $\delta^{13}C$ signature of OM in 0–30 cm depth and the mean $\delta^{13}C$ signature of CH_4 in 20 and 30 cm depth for the mixing model. We used the mean fractionation factor for methane oxidation in peat at 0–20 cm depth (Δ = 54.0‰) and across three incubation temperatures (5, 10 and 15 °C) as the statistical test showed no significant effect of neither depth nor temperature. The fractionation factors are subtracted from the $\delta^{13}C_{CH4,pw}$ because the oxidation of CH_4 discriminates against the heavy isotope (^{13}C) and thus the resulting CO_2 is depleted in ^{13}C compared to the source CH_4. In other words, the $\delta^{13}C$ signature of the CO_2 produced during CH_4 oxidation is more negative than the source CH_4.

The relative contribution of CH_4 oxidation ($\%CH_{4oxi}$) is calculated as [36]:

$$\%CH_{4oxi} = \frac{\text{Oxidized } CH_4 \text{ flux}}{\text{Oxidized } CH_4\text{flux} + \text{measured } CH_4\text{flux}} * 100, \quad (5)$$

and the oxidized CO_2 flux is calculated by multiplying f_{CH4} and R_h.

2.9. Data Presentation and Statistics

The differences in fractionation factor between the four depths, and three temperatures were tested with a mixed linear model in R version 3.5.1 (R Core Team, Vienna, Austria) using depth and temperature as fixed effects and core as random effect. The model was reduced stepwise using ANOVA.

All data are presented as mean and standard error. Means and errors for the time series of relative contribution of CH_4 oxidation to R_h as well as time series of isotopic signatures of ER and R_h are weighted averages based on the four-hour averages, as some missing values during nighttime would skew an overall average towards daytime values. Figures were made in Sigmaplot 13.0 (Systat Software Inc., San Jose, CA, USA) and R.

3. Results and Discussion

3.1. Isotopic Signatures of CO_2 Fluxes

Measurements of mass- and isofluxes of ER and R_h as well as fluxes of NEE and CH_4 from the undisturbed plots in the mire were carried out from 18 to 27 July 2014 (Figure 1 and Figure S1). During this period, the water table level dropped from 0.08 to 0.16 m below mire surface, and the average daily air temperature at 10 cm above mire surface varied between 8.2 and 30.9 °C (Figure S2). The $\delta^{13}C$ signature of source CO_2 in both the ER and R_h fluxes showed strong diurnal cycles (Figure 1). The $\delta^{13}C$ signature of ER ($\delta^{13}C_{ER}$) varied between −52 and −22‰ with minimum values occurring during mid-day. The average of $\delta^{13}C_{ER}$ for the period was -32.3 ± 1.0‰ (±standard error). The four-hour means of $\delta^{13}C$ signature of R_h ($\delta^{13}C_{Rh}$) usually peaked at 2 am (Figure 1b) with a maximum $\delta^{13}C_{Rh}$ of −22‰, whereas the minimum $\delta^{13}C_{Rh}$ was −99‰. Average $\delta^{13}C_{Rh}$ was -49.2 ± 2.3‰.

The observed diurnal pattern of $\delta^{13}C_{ER}$ indicates that given the less depleted source during night, ER mainly results from OM mineralization, whereas during the day, the more depleted signatures of CO_2 suggest an additional process contributing to ER. This trend is even more apparent in the vegetation-free R_h plots. We suggest that the source of these negative $\delta^{13}C$ values is the result of methanotrophs oxidizing CH_4 with an average $\delta^{13}C$ of −67.2‰ (see below) in the peat pore water.

The fact that some $\delta^{13}C_{Rh}$ values were lower than the average $\delta^{13}C$ signature of the CH_4 may be due to the uncertainty associated with the estimation of the keeling intercepts (the standard error of the intercept is on average 8.3‰ for R_h) or a small difference in $\delta^{13}C_{CH4,pw}$ between the 2014 measurement period and the pore water sampling done in 2015. However, it is also likely due to a large contribution from CH_4 oxidation and the fractionation occurring during the oxidation process, which lowers the $\delta^{13}C$ signatures of the resulting CO_2 relative to the substrate CH_4 [33].

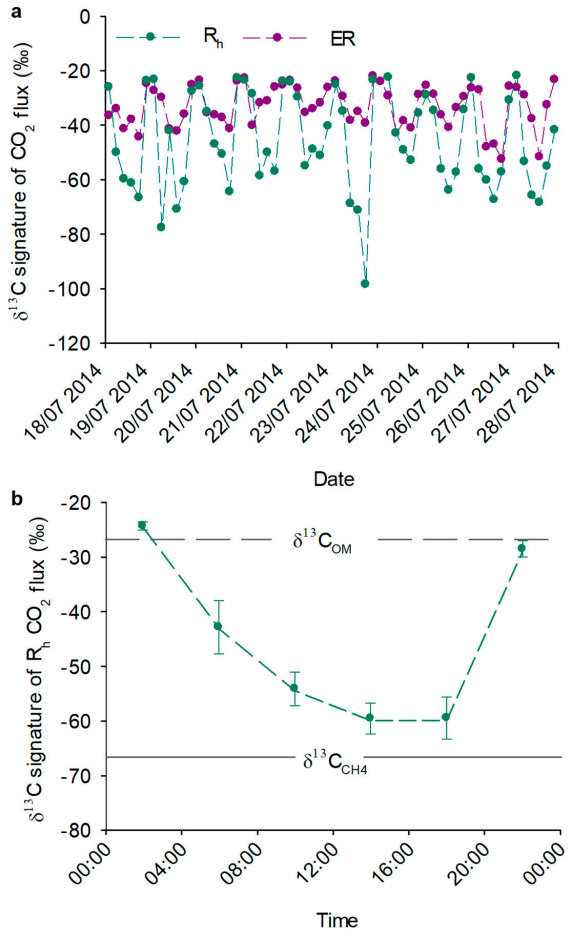

Figure 1. (**a**) Four-hourly averages of the carbon isotopic signatures of ecosystem respiration (ER) and heterotrophic respiration (R_h) and (**b**) average diurnal variation during 18 to 27 July 2014 in the isotopic signature of CO_2 fluxes from the R_h plots (i.e., plots that had all photosynthetic biomass removed). Error bars in (**b**) show standard error. Dashed and solid lines in (**b**) show respectively the $\delta^{13}C$ signatures of organic matter ($\delta^{13}C_{OM}$) and pore water CH_4 ($\delta^{13}C_{CH4,pw}$) in the peatland. The lines connecting the points are visual aids.

3.2. Mixing Model

We used a two-source mixing model to quantify the relative contributions of OM mineralization and CH_4 oxidation to total R_h fluxes. The $\delta^{13}C$ signature of OM ($\delta^{13}C_{OM}$) integrated over 0 to 30 cm depth was −27.4‰ (Figure S3) and was used to represent the $\delta^{13}C$ signature of OM mineralization in the mixing model. The average $\delta^{13}C$ signature of the pore water CH_4 ($\delta^{13}C_{CH4,pw}$) was −67.2‰ and represents the $\delta^{13}C$ signature of CO_2 originating from CH_4 oxidation in the mixing model. We consider the $\delta^{13}C_{CH4,pw}$ in 2015 a good representation of the $\delta^{13}C_{CH4,pw}$ from 2014 due to little variation between years in these depths below the water table (−73.4 ± 0.5‰ on 8 August 2017 and −68.1 ± 0.6‰ on 26 July 2018). In order to account for the fractionation taking place when CH_4 is oxidized to CO_2, we subtracted the measured fractionation factor Δ = 54.0 ± 3.4‰ (n = 28) from the $\delta^{13}C_{CH4,pw}$

(Figure S4). Our fractionation factor is within the range reported in the literature [19,24,33,37–39] though slightly on the high end. Over the measurement period (18 to 27 July 2014) CH_4 oxidation contributed 20 ± 2.5% of R_h (Figure 2a) and 10 ± 0.5% of ER (Figure S1, assuming that no additional oxidation occurs in vegetated plots due to production and transport of oxygen by plants). At the same time, if ignoring any difference in transport rate between CH_4 and CO_2, 74% of the produced CH_4 in the R_h plots were oxidized to CO_2 within the assessed time period. We made a sensitivity analysis to assess the effect of the calculated contribution of CH_4 oxidation to R_h using the minimum and maximum measured $\delta^{13}C_{OM}$ and $\delta^{13}C_{CH4,pw}$ as well as minimum and maximum fractionation factors from the literature (Figures S7 and S8). The analysis showed that the highest and lowest estimates across this period resulted in methane oxidation contributing between 16 and 57% of R_h. Our result (20%) is therefore in the lower range, making it more likely that we underestimate the relative contribution of methane oxidation to soil CO_2 effluxes. Using this novel approach our results showed that during a relatively warm and dry period (Figure S2), CH_4 oxidation likely reduced CH_4 emissions and contributed considerably to R_h in this boreal peatland. Although our approach appears promising in quantifying methane oxidation in real time in the field, our results also stress that more high-frequency measurements are needed to quantify the importance of this process for various mire plant communities and during various stages of the growing season associated with differences in plant phenology, water table levels, and soil temperatures.

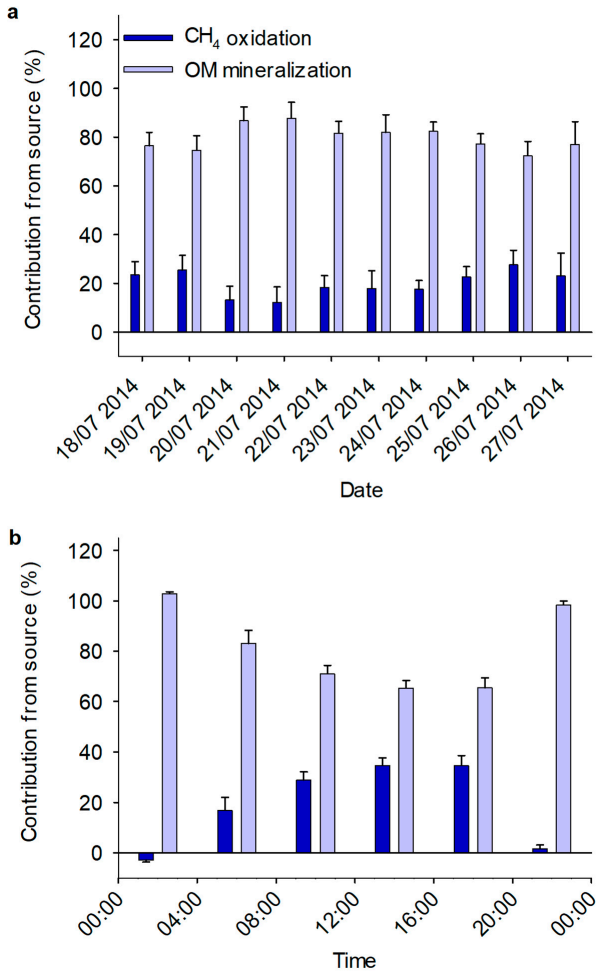

Figure 2. The relative contribution of CH_4 oxidation and organic matter (OM) mineralization to heterotrophic respiration for the period 18 to 27 July 2014 shown as (**a**) daily averages and (**b**) diurnal ensembles. Error bars show standard error. The negative contribution from CH_4 oxidation to R_h at 2 am is an artifact of uncertainty in the estimation.

3.3. Diurnal Variation

We also observed a diurnal variation in the relative contribution of CH_4 oxidation to total CO_2 efflux from the R_h plots (Figure 2b). Previously, speculations around diurnal variation in peatland CH_4 oxidation have been inferred based on diurnal variation of CH_4 fluxes [40]. However, this study shows diurnal variation the isotopic signature of R_h and thus likely in CH_4 oxidation. During nighttime, the contribution of CH_4 oxidation to R_h seemed negligible, while during the day, CH_4 oxidation appeared to contribute up to 35 ± 3.0%. In order to assess whether the diurnal variation was caused by a change in CH_4 oxidation rather than increased OM mineralization during night, we calculated the CO_2 fluxes associated with the two processes (Figure S5). These fluxes show that even though mineralization like total R_h appears to be higher during night, there still seems to be a distinct diurnal pattern in the CH_4 oxidation. We suggest that the diurnal variation is driven by a combination of changes in soil temperature (on average 7.1 and 2.6 °C difference between min. and max. temperatures in 2 and 10 cm depth respectively, Figure S2) and a decreasing water table. The water table follows a staircase-like trend with lowering during day and plateauing at night (Figure S2) and is likely driven by enhanced evapotranspiration during the day. This would lead to daytime O_2 intrusion into areas in the soil profile with high CH_4 concentration (enhancing CH_4 oxidation rates), as well as to the possible release of CO_2 with a depleted signature (originating from CH_4) due to enhanced diffusion rates [41]. It is important to point out that the diurnal variation in the isotopic signature of CO_2 from vegetated plots may also partly be caused by increased input of O_2 to the rhizosphere by photosynthesizing plants. Although it was beyond the scope of this study, the observed diurnal variation in methane oxidation highlights the need for depth specific O_2 and CH_4 measurements in order to better understand the drivers responsible for temporal variation in methane oxidation in the field. The diurnal variation in $\delta^{13}C$ signatures of R_h also highlights that bias in the diurnal sampling protocol can influence the results as e.g., only daytime sampling would give values highly biased towards more depleted $\delta^{13}C$ signatures. It should also be noted, that there was a buildup of CO_2 and CH_4 in the air above the mire surface during each night of the measurement period, which may have led to some overestimation of the flux isotopic signature [42,43] (see Figure S6).

Our results show that CH_4 oxidation may contribute considerably to R_h fluxes, and thus highlights the importance of including this process in peatland CO_2 models in order to better predict and understand peatland C dynamics. Our new approach for measuring CH_4 oxidation creates the opportunity for future studies to provide the necessary data to validate and improve these models. Furthermore, studies estimating ecosystem respiration in boreal peatlands based on partitioning of eddy covariance data assume that OM mineralization and plant respiration are the only sources for respired CO_2 and commonly relate ecosystem respiration to only one factor; namely temperature [44,45]. However, our results show that in peatland ecosystems a considerable amount of R_h fluxes could be derived from CH_4 oxidation which is controlled by additional factors (e.g., water table level [46] and CH_4 and O_2 availability [47]), that differ from the main factors controlling OM mineralization and plant respiration.

3.4. Methodological Limitations

In our two-source mixing model, we assume that fractionation during diffusion of CH_4 and CO_2 would not strongly influence our results for the following reasons (1) our estimates of the source $\delta^{13}C$ signatures integrate over the soil profile, (2) there was no difference in the $\delta^{13}C_{CH4,pw}$ at depths 20 and 30 cm, and (3) CH_4 diffusion in water saturated soil causes negligible fractionation [24] and in addition other non-fractionating transport processes such as pressure gradients and near surface layer air flow might have contributed to the total flux [48]. We also assume that OM mineralization and aerobic CH_4 oxidation are the only two processes influencing the isotopic signature of $^{13}CO_2$ from the R_h plots. Although it is possible that anaerobic CH_4 oxidation could potentially take place [49,50], we consider this process of minor importance in this nutrient-poor ecosystem. However, if anaerobic CH_4 oxidation was occurring, it would produce CH_4 less depleted in ^{13}C due to a lower fractionation factor [50] and thereby, if anything, our estimates of contribution of CH_4 oxidation to total R_h would

be underestimated. We also acknowledge that CO_2 is produced during methanogenesis. Theoretically, both hydrogenotrophic (based on carbohydrate fermentation and including the step of H_2 production) and acetoclastic methanogenesis produces equimolar amounts of CO_2 and CH_4, and as the CH_4 is depleted compared to the substrate, the CO_2 must be equally enriched [51]. An estimation by Corbett and colleagues [51] based on a substrate signature of −26‰ and a resulting CH_4 signature of −60‰, suggested a ^{13}C signature of 8‰ for the CO_2 produced during methanogenesis [51]. In the current study, we were not able to include the CO_2 from methanogenesis in our mixing model, and therefore our estimation of the contribution of CH_4 oxidation to total R_h is potentially underestimated. This is because the CO_2 from methanogenesis raises the isotopic signature of the total pore water CO_2 pool and emitted CO_2 and thereby causes the contribution from CH_4 oxidation to appear smaller.

We used the method of plant removal and plot trenching for estimating R_h [52]. As is the case for other methods measuring R_h, this approach has some shortcomings. For instance, the removal of the vegetation causes a reduction in supply of rhizodeposits and possibly a lower input of O_2 to the soil (due to elimination of downward plant mediated transport of O_2). For CH_4 oxidation, the latter is mostly relevant when the water table is high and thus limits the diffusion of O_2 from the atmosphere into soil, as was not the case during our measurement campaign. The decrease in concentration of both O_2 and rhizodeposits may however be counteracted to some extent by lateral transfer with moving water, and we consider this issue of minor importance in our study. The plant removal in the R_h plot also eliminated CH_4 transport by plants, and thus the CH_4 fluxes from these plots were on average 16% lower than from the vegetated plots. In addition, the potential for CH_4 oxidization in the vegetation-free plots might also be somewhat lower to due to the removal of the upper moss layer with its associated methanotrophic communities [53]. However, the oxidation in these plots was on average 74% of potential fluxes, which is marginally higher than the 70% oxidation in vegetated plots, and thus we would argue that vascular plant CH_4 transport and moss-associated CH_4 oxidation plays only a minor role for net CH_4 oxidation in our experiment.

In this study we used an average of the measured fractionation factors across peat depth and incubation temperature as we found no statistical effect of these parameters. We did, however, find a correlation between oxidation rate and fractionation factor (Figure S9), although we were not able to include this information into the mixing model at this point, as we are using the model to estimate the oxidation rate. We acknowledge however that the fractionation factor can vary in response to different parameters such as CH_4 concentration and CH_4 oxidation rate [54,55]. The fractionation factor may be positively correlated with CH_4 starting concentration of in incubations [54] highlighting the importance of matching the CH_4 starting concentration of incubations with conditions found in the field. The fractionation factor is also influenced by the fraction of active methanotrophs [55] and thus a decreasing water table could initially influence the fractionation factor when exposing potentially dormant methanotrophs to optimal conditions. However, according to our sensitivity analysis (Figure S8) this factor alone cannot explain the observed diurnal variation in CH_4 oxidation. We encourage future studies for improvements on this method by including this component.

4. Conclusions

In this study, we present a new method for continuous, high-frequency *in-situ* quantification of CH_4 oxidation in peatlands. Previous studies from wetlands and lakes have quantified CH_4 oxidation using the $\delta^{13}C$ (and δD) of pore water or lake water CH_4 [19,33,37] and CH_4 flux [56]. However, our method is the first, to our knowledge, that uses high temporal resolution isotopic measurements of $^{13}CO_2$ in R_h fluxes based on automated chamber measurements on vegetation-free plots to quantify the relative contribution of CH_4 oxidation to the heterotrophic and ecosystem respiration fluxes in the field. Thus, our approach creates an unprecedented opportunity to study the temporal dynamics and controls of CH_4 oxidation in peatland ecosystems. In addition, we observed a diurnal pattern in the $\delta^{13}C$ signatures of heterotrophic respiration suggesting a high contribution of CH_4 oxidation to CO_2 fluxes during daytime and a negligible contribution during nighttime. Overall, our novel approach

of directly measuring the isotopic composition of R_h at high temporal resolution provides unique insight into the effect of CH_4 oxidation on CO_2 and CH_4 fluxes, which is crucial for further developing process-based models and improving our understanding of peatland C dynamics.

Supplementary Materials: The following are available online at http://www.mdpi.com/2571-8789/3/1/4/s1, Figure S1. CO_2 and CH_4 fluxes, Figure S2. PAR, temperature and water table data, Figure S3. Carbon isotopic signature of peat, Figure S4. Fractionation factors, Figure S5. CO_2 fluxes from CH_4 oxidation and OM mineralization, Figure S6. Ambient air CO_2 concentrations and isotopic signatures, Figure S7. Sensitivity analysis of daily averages, Figure S8. Sensitivity analysis of hourly averages, Figure S9. Correlation between fractionation factor and oxidation rate, Table S1. Sensitivity analysis of contribution of CH_4 oxidation to heterotrophic respiration.

Author Contributions: Conceptualization, N.J.H., M.B.N., M.Ö. and M.P.; Formal analysis, C.S.N., N.J.H. and J.J.; Funding acquisition, M.B.N.; Investigation, C.S.N., N.J.H. and M.P.; Methodology, C.S.N., N.J.H., M.B.N., M.Ö. and M.P.; Visualization, C.S.N.; Writing—original draft, C.S.N.; Writing—review & editing, C.S.N., N.J.H., M.B.N., M.Ö., J.J. and M.P.

Funding: This research was funded by the Kempe Foundation, grant number JCK-1608 and Carl Tryggers Foundation grant number CTS 15-377.

Acknowledgments: We kindly acknowledge support from the ICOS Sweden (Integrated Carbon Observation System) and SITES (Swedish Infrastructure for Ecosystem Research) research infrastructure funded by the Swedish Research Council and partner research institutes.

Conflicts of Interest: The authors declare no conflict of interest.

References

1. Loisel, J.; Yu, Z.C.; Beilman, D.W.; Camill, P.; Alm, J.; Amesbury, M.J.; Anderson, D.; Andersson, S.; Bochicchio, C.; Barber, K.; et al. A database and synthesis of northern peatland soil properties and Holocene carbon and nitrogen accumulation. *Holocene* **2014**, *24*, 1028–1042. [CrossRef]
2. Christensen, T.R.; Ekberg, A.; Ström, L.; Mastepanov, M.; Panikov, N.; Öquist, M.; Svensson, B.H.; Nykanen, H.; Martikainen, P.J.; Oskarsson, H. Factors controlling large scale variations in methane emissions from wetlands. *Geophys. Res. Lett.* **2003**, *30*. [CrossRef]
3. McCalley, C.K.; Woodcroft, B.J.; Hodgkins, S.B.; Wehr, R.A.; Kim, E.H.; Mondav, R.; Crill, P.M.; Chanton, J.P.; Rich, V.I.; Tyson, G.W.; et al. Methane dynamics regulated by microbial community response to permafrost thaw. *Nature* **2014**, *514*, 478–481. [CrossRef] [PubMed]
4. Granberg, G.; Mikkela, C.; Sundh, I.; Svensson, B.H.; Nilsson, M. Sources of spatial variation in methane emission from mires in northern Sweden: A mechanistic approach in statistical modeling. *Glob. Biogeochem. Cycle* **1997**, *11*, 135–150. [CrossRef]
5. Wu, Y.Q.; Verseghy, D.L.; Melton, J.R. Integrating peatlands into the coupled Canadian Land Surface Scheme (CLASS) v3.6 and the Canadian Terrestrial Ecosystem Model (CTEM) v2.0. *Geosci. Model Dev.* **2016**, *9*, 2639–2663. [CrossRef]
6. Wu, J.H.; Roulet, N.T.; Nilsson, M.; Lafleur, P.; Humphreys, E. Simulating the Carbon Cycling of Northern Peat lands Using a Land Surface Scheme Coupled to a Wetland Carbon Model (CLASS3W-MWM). *Atmos.-Ocean* **2012**, *50*, 487–506. [CrossRef]
7. Abdalla, M.; Hastings, A.; Bell, M.J.; Smith, J.U.; Richards, M.; Nilsson, M.B.; Peichl, M.; Lofvenius, M.O.; Lund, M.; Helfter, C.; et al. Simulation of CO_2 and Attribution Analysis at Six European Peatland Sites Using the ECOSSE Model. *Water Air Soil Poll.* **2014**, *225*, 14. [CrossRef]
8. Qiu, C.; Zhu, D.; Ciais, P.; Guenet, B.; Krinner, G.; Peng, S.; Aurela, M.; Bernhofer, C.; Brümmer, C.; Bret-Harte, S.; et al. ORCHIDEE-PEAT (revision 4596), a model for northern peatland CO_2, water and energy fluxes on daily to annual scales. *Geosci. Mod. Dev. Discuss.* **2017**. [CrossRef]
9. Metzger, C.; Nilsson, M.B.; Peichl, M.; Jansson, P.E. Parameter interactions and sensitivity analysis for modelling carbon heat and water fluxes in a natural peatland, using CoupModel v5. *Geosci. Model Dev.* **2016**, *9*, 4313–4338. [CrossRef]
10. Gerard, G.; Chanton, J. Quantification of methane oxidation in the rhizosphere of emergent aquatic macrophytes: Defining upper limits. *Biogeochemistry* **1993**, *23*, 79–97. [CrossRef]

11. Kankaala, P.; Bergström, I. Emission and oxidation of methane in *Equisetum fluviatile* stands growing on organic sediment and sand bottoms. *Biogeochemistry* **2004**, *67*, 21–37. [CrossRef]
12. Sundh, I.; Mikkela, C.; Nilsson, M.; Svensson, B.H. Potential Aerobic Methane Oxidation in a Sphagnum-Dominated Peatland—Controlling Factors and Relation to Methane Emission. *Soil Biol. Biochem.* **1995**, *27*, 829–837. [CrossRef]
13. Ding, W.X.; Cai, Z.C.; Tsuruta, H. Factors affecting seasonal variation of methane concentration in water in a freshwater marsh vegetated with *Carex lasiocarpa*. *Biol. Fert. Soils* **2005**, *41*, 1–8. [CrossRef]
14. Lombardi, J.E.; Epp, M.A.; Chanton, J.P. Investigation of the methyl fluoride technique for determining rhizospheric methane oxidation. *Biogeochemistry* **1997**, *36*, 153–172. [CrossRef]
15. van der Nat, F.; Middelburg, J.J. Seasonal variation in methane oxidation by the rhizosphere of *Phragmites australis* and *Scirpus lacustris*. *Aquat. Bot.* **1998**, *61*, 95–110. [CrossRef]
16. Popp, T.J.; Chanton, J.P.; Whiting, G.J.; Grant, N. Methane stable isotope distribution at a *Carex* dominated fen in north central Alberta. *Glob. Biogeochem. Cycle* **1999**, *13*, 1063–1077. [CrossRef]
17. Groot, T.T.; Bodegom, P.M.V.; Harren, F.J.M.; Meijer, H.A.J. Quantification of methane oxidation in the rice rhizosphere using ^{13}C-labelled methane. *Biogeochemistry* **2003**, *64*, 355–372. [CrossRef]
18. Riveros-Iregui, D.A.; King, J.Y. Isotopic Evidence of Methane Oxidation across the Surface Water-Ground Water Interface. *Wetlands* **2008**, *28*, 928–937. [CrossRef]
19. Cadieux, S.B.; White, J.R.; Sauer, P.E.; Peng, Y.B.; Goldman, A.E.; Pratt, L.M. Large fractionations of C and H isotopes related to methane oxidation in Arctic lakes. *Geochim. Cosmochim. Acta* **2016**, *187*, 141–155. [CrossRef]
20. Fechner, E.J.; Hemond, H.F. Methane transport and oxidation in the unsaturated zone of a Sphagnum peatland. *Glob. Biogeochem. Cycles* **1992**, *6*, 33–44. [CrossRef]
21. Urmann, K.; Gonzalez-Gil, G.; Schroth, M.H.; Zeyer, J. Quantification of Microbial Methane Oxidation in an Alpine Peat Bog. *Vadose Zone J.* **2007**, *6*, 705–712. [CrossRef]
22. King, G.M. In situ analyses of methane oxidation associated with the roots and rhizomes of a bur reed, *Sparganium eurycarpum*, in a Maine wetland. *Appl. Environ. Microbiol.* **1996**, *62*, 4548–4555. [PubMed]
23. Popp, T.J.; Chanton, J.P.; Whiting, G.J.; Grant, N. Evaluation of methane oxidation in the rhizosphere of a *Carex* dominated fen in north central Alberta, Canada. *Biogeochemistry* **2000**, *51*, 259–281. [CrossRef]
24. Preuss, I.; Knoblauch, C.; Gebert, J.; Pfeiffer, E.M. Improved quantification of microbial CH_4 oxidation efficiency in arctic wetland soils using carbon isotope fractionation. *Biogeosciences* **2013**, *10*, 2539–2552. [CrossRef]
25. Alexandersson, H.; Karlström, C.; Larsson-Mccann, S. *Temperature and Precipitation in Sweden during 1961–1990. Reference Normals*; SMHI Meteorologi: Norrköping, Sweden, 1991; Volume 81.
26. Peichl, M.; Öquist, M.; Löfvenius, M.O.; Ilstedt, U.; Sagerfors, J.; Grelle, A.; Lindroth, A.; Nilsson, M.B. A 12-year record reveals pre-growing season temperature and water table level threshold effects on the net carbon dioxide exchange in a boreal fen. *Environ. Res. Lett.* **2014**, *9*, 11. [CrossRef]
27. Eriksson, T.; Öquist, M.G.; Nilsson, M.B. Effects of decadal deposition of nitrogen and sulfur, and increased temperature, on methane emissions from a boreal peatland. *J. Geophys. Res.-Biogeosci.* **2010**, *115*, 13. [CrossRef]
28. Nilsson, M.; Sagerfors, J.; Buffam, I.; Laudon, H.; Eriksson, T.; Grelle, A.; Klemedtsson, L.; Weslien, P.; Lindroth, A. Contemporary carbon accumulation in a boreal oligotrophic minerogenic mire—A significant sink after accounting for all C-fluxes. *Glob. Chang. Biol.* **2008**, *14*, 2317–2332. [CrossRef]
29. Laine, A.M.; Bubier, J.; Riutta, T.; Nilsson, M.B.; Moore, T.R.; Vasander, H.; Tuittila, E.-S. Abundance and composition of plant biomass as potential controls for mire net ecosytem CO_2 exchange. *Botany* **2011**, *90*, 63–74. [CrossRef]
30. Järveoja, J.; Nilsson, M.B.; Gažovič, M.; Crill, P.M.; Peichl, M. Partitioning of the net CO_2 exchange using an automated chamber system reveals plant phenology as key control of production and respiration fluxes in a boreal peatland. *Glob. Chang. Biol.* **2018**, *24*, 3436–3451. [CrossRef]
31. Eriksson, T.; Öquist, M.G.; Nilsson, M.B. Production and oxidation of methane in a boreal mire after a decade of increased temperature and nitrogen and sulfur deposition. *Glob. Change Biol.* **2010**, *16*, 2130–2144. [CrossRef]

32. Keeling, C.D. The Concentration and Isotopic Abundances of Atmospheric Carbon Dioxide in Rural Areas. *Geochim. Cosmochim. Acta* **1958**, *13*, 322–334. [CrossRef]
33. Happell, J.D.; Chanton, J.P.; Showers, W.S. The Influence of Methane Oxidation on the Stable Isotopic Composition of Methane Emitted from Florida Swamp Forests. *Geochim. Cosmochim. Acta* **1994**, *58*, 4377–4388. [CrossRef]
34. Coleman, D.D.; Risatti, J.B.; Schoell, M. Fractionation of Carbon and Hydrogen Isotopes by Methane-Oxidizing Bacteria. *Geochim. Cosmochim. Acta* **1981**, *45*, 1033–1037. [CrossRef]
35. Fry, B. *Stable Isotope Ecology*; Springer: New York, NY, USA, 2006; p. 316.
36. Schipper, L.A.; Reddy, K.R. Determination of methane oxidation in the rhizosphere of *Sagittaria lancifolia* using methyl fluoride. *Soil Sci. Soc. Am. J.* **1996**, *60*, 611–616. [CrossRef]
37. Kankaala, P.; Taipale, S.; Nykanen, H.; Jones, R.I. Oxidation, efflux, and isotopic fractionation of methane during autumnal turnover in a polyhumic, boreal lake. *J. Geophys. Res.-Biogeosci.* **2007**, *112*. [CrossRef]
38. De Visscher, A.; De Pourcq, I.; Chanton, J. Isotope fractionation effects by diffusion and methane oxidation in landfill cover soils. *J. Geophys. Res.-Atmos.* **2004**, *109*, 8. [CrossRef]
39. Reeburgh, W.S.; Hirsch, A.I.; Sansone, F.J.; Popp, B.N.; Rust, T.M. Carbon kinetic isotope effect accompanying microbial oxidation of methane in boreal forest soils. *Geochim. Cosmochim. Acta* **1997**, *61*, 4761–4767. [CrossRef]
40. Mikkelä, C.; Sundh, I.; Svensson, B.H.; Nilsson, M. Diurnal variation in methane emission in relation to the water table, soil temperature, climate and vegetation cover in a Swedish acid mire. *Biogeochemistry* **1995**, *28*, 93–114. [CrossRef]
41. Moore, T.R.; Dalva, M. The influence of temperature and water table position on carbon dioxide and methane emissions from laboratory columns of peatland soils. *J. Soil Sci.* **1993**, *44*, 651–664. [CrossRef]
42. van Asperen, H.; Warneke, T.; Sabbatini, S.; Höpker, M.; Nicolini, G.; Chiti, T.; Papale, D.; Böhm, M.; Notholt, J. Diel variation in isotopic composition of soil respiratory CO_2 fluxes: The role of non-steady state conditions. *Agric. For. Meteorol.* **2017**, *234–235*, 95–105. [CrossRef]
43. Braendholt, A.; Larsen, K.S.; Ibrom, A.; Pilegaard, K. Overestimation of closed-chamber soil CO_2 effluxes at low atmospheric turbulence. *Biogeosciences* **2017**, *14*, 1603–1616. [CrossRef]
44. Lasslop, G.; Reichstein, M.; Papale, D.; Richardson, A.D.; Arneth, A.; Barr, A.; Stoy, P.; Wohlfahrt, G. Separation of net ecosystem exchange into assimilation and respiration using a light response curve approach: Critical issues and global evaluation. *Glob. Chang. Biol.* **2010**, *16*, 187–208. [CrossRef]
45. Reichstein, M.; Falge, E.; Baldocchi, D.; Papale, D.; Aubinet, M.; Berbigier, P.; Bernhofer, C.; Buchmann, N.; Gilmanov, T.; Granier, A.; et al. On the separation of net ecosystem exchange into assimilation and ecosystem respiration: Review and improved algorithm. *Glob. Chang. Biol.* **2005**, *11*, 1424–1439. [CrossRef]
46. Roslev, P.; King, G.M. Regulation of methane oxidation in a freshwater wetland by water table changes and anoxia. *FEMS Microbiol. Ecol.* **1996**, *19*, 105–115. [CrossRef]
47. Lai, D.Y.F. Methane Dynamics in Northern Peatlands: A Review. *Pedosphere* **2009**, *19*, 409–421. [CrossRef]
48. Redeker, K.R.; Baird, A.J.; Teh, Y.A. Quantifying wind and pressure effects on trace gas fluxes across the soil–atmosphere interface. *Biogeosciences* **2015**, *12*, 7423–7434. [CrossRef]
49. Smemo, K.A.; Yavitt, J.B. Anaerobic oxidation of methane: An underappreciated aspect of methane cycling in peatland ecosystems? *Biogeosciences* **2011**, *8*, 779–793. [CrossRef]
50. Smemo, K.A.; Yavitt, J.B. Evidence for Anaerobic CH_4 Oxidation in Freshwater Peatlands. *Geomicrobiol. J.* **2007**, *24*, 583–597. [CrossRef]
51. Corbett, J.E.; Tfaily, M.M.; Burdige, D.J.; Cooper, W.T.; Glaser, P.H.; Chanton, J.P. Partitioning pathways of CO_2 production in peatlands with stable carbon isotopes. *Biogeochemistry* **2013**, *114*, 327–340. [CrossRef]
52. Bond-Lamberty, B.; Bronson, D.; Bladyka, E.; Gower, S.T. A comparison of trenched plot techniques for partitioning soil respiration. *Soil Biol. Biochem.* **2011**, *43*, 2108–2114. [CrossRef]
53. Larmola, T.; Tuittila, E.S.; Tiirola, M.; Nykanen, H.; Martikainen, P.J.; Yrjala, K.; Tuomivirta, T.; Fritze, H. The role of Sphagnum mosses in the methane cycling of a boreal mire. *Ecology* **2010**, *91*, 2356–2365. [CrossRef] [PubMed]
54. Teh, Y.A.; Silver, W.L.; Conrad, M.E.; Borglin, S.E.; Carlson, C.M. Carbon isotope fractionation by methane-oxidizing bacteria in tropical rain forest soils. *J. Geophys. Res.-Biogeosci.* **2006**, *111*. [CrossRef]

55. Templeton, A.S.; Chu, K.-H.; Alvarez-Cohen, L.; Conrad, M.E. Variable carbon isotope fractionation expressed by aerobic CH_4-oxidizing bacteria. *Geochim. Cosmochim. Acta* **2006**, *70*, 1739–1752. [CrossRef]
56. Dorodnikov, M.; Marushchak, M.; Biasi, C.; Wilmking, M. Effect of microtopography on isotopic composition of methane in porewater and efflux at a boreal peatland. *Boreal Environ. Res.* **2013**, *18*, 269–279.